THE JOURNAL OF PHYSICAL CHEMISTRY B

Article

A Study of the Impact of Polyanions on the Formation of Lipid Bilayers on Top of Polyelectrolyte Multilayers with Poly(allylamine hydrochloride) as Top Layer

Eleftheria Diamanti, Patrizia Andreozzi, Christopher Kirby, Ramiro Anguiano, Luis Yate, Hendrik Heinz, Ronald F. Ziolo, Edwin Donath, and Sergio Enrique Moya

J. Phys. Chem. B, **Just Accepted Manuscript** • DOI: 10.1021/acs.jpcb.6b12237 • Publication Date (Web): 13 Jan 2017

ACS Publications

The Journal of Physical Chemistry B is published by the American Chemical Society. 1155 Sixteenth Street N.W., Washington, DC 20036

A Study of the Impact of Polyanions on the Formation of Lipid Bilayers on Top of Polyelectrolyte Multilayers with Poly(allylamine hydrochloride) as Top Layer

*Eleftheria Diamanti[1], Patrizia Andreozzi[1], Christopher Kirby[2], Ramiro Anguiano[3], Luis Yate[1], Hendrik Heinz[2], Ronald F. Ziolo[2,3], Edwin Donath[4], Sergio Enrique Moya[1]**

[1]Soft Matter Nanotechnology Group, CIC biomaGUNE, Paseo Miramón 182 C, 20009 San Sebastian, Guipuzcoa, Spain.

[2]Department of Chemical and Biological Engineering, University of Colorado Boulder, 3415 Colorado Avenue Boulder, CO 80309-0596 Colorado, United States of America.

[3]Departamento de Materiales Avanzados, Centro de Investigación en Química Aplicada, Blvd. Enrique Reyna Hermosillo No.140, 25250 Saltillo, Coahuila México.

[4]Institute of Biophysics and Medical Physics, Faculty of Medicine, University of Leipzig, 04107 Leipzig, Germany.

*Corresponding author: smoya@cicbiomagune.es

Abstract

The role of the polyanion on the formation of lipid bilayers on top of polyelectrolyte multilayers (PEMs) with poly(allylamine hydrochloride) (PAH) as top layer is studied for the deposition of vesicles of mixed lipid composition, 50:50 molar ratio of the zwitterionic 1,2-Dioleoyl-sn-glycero-3-phosphocholine (DOPC) and negatively charged 1,2-dioleoyl-sn-glycero-3-phospho-L-serine (DOPS). PEMs are assembled with poly(sodiumstyrene sulfonate) (PSS), poly(acrylic acid) (PAA) and alginic acid sodium salt (Alg) as polyanions. The assembly of the vesicles on the PEMs is followed by means of the Quartz Crystal Microbalance with Dissipation (QCMD). Fluorescence Recovery after Photobleaching (FRAP) measurements are applied to evaluate bilayer formation. While a bilayer is formed on top of PAH/PSS multilayers, the vesicles are adsorbed on top of PAH/Alg and PAH/PAA multilayers, remaining unruptured or only partially fused. The influence of the surface composition of the PEMs *vs* bulk properties is analyzed. Phosphate ions present in phosphate buffered saline (PBS) play a fundamental role in bilayer formation on top of PAH/PSS as they complex to the PAH and render the surface potential close to zero. For PAH/PAA and PAH/Alg PBS renders the surface negative. X-Ray Photoelectron Spectroscopy show that the dibasic phosphate ions from PBS complex preferentially to PAH in PAH/PAA and PAH/Alg multilayers while monobasic phosphates complex to PAH in PAH/PSS. An explanation for the absence of bilayer formation on PAH/PAA and PAH/Alg is given based on the different affinity of phosphate ions for PAH in combination with the different polyanions.

Introduction

Supported lipid bilayers have been extensively studied as model membranes in biophysical studies or as part of sensors and in biotechnology[1–7]. A diversity of solid materials such as silica, titania, mica etc[3,8–10] have been employed as bilayer supports. Comparatively, significantly less work has been performed on soft interfaces as supports for lipid bilayers. Lipid bilayers deposited on a soft polymer cushion such as polyelectrolyte multilayer (PEM) films are of particular interest since in nature, cellular membranes are supported by a soft cushion of proteins and carbohydrates[11,12,13]. PEMs are especially interesting as supports due to their simple and step-forward assembly based on the alternating deposition of oppositely charged polyelectrolytes, mainly triggered by electrostatic interactions[14,15]. Although some studies have been conducted on the assembly of lipid bilayers on top of PEMs, there is still a lack of knowledge over the complete mechanism of bilayer formation. In most of the reported works, lipid assembly on top of PEMs results in non-fused vesicles, incomplete membranes or in membranes with large defects (pores)[11]. Fischlechner et al. have shown bilayer assembly on top of 11 layers of polyallylamine hydrochloride (PAH) and polystyrene sulfonate (PSS) from vesicles of mixed lipid composition, 50:50 molar ratio of the zwitterionic phosphatidylcholine (DOPC) and negatively charged phosphatidylserine (DOPS)[16]. Moreover, the authors showed that the mechanism followed for the formation of the bilayer is based on the adsorption of vesicles onto the PEM surface, their subsequent rupture and fusion to finally form a complete and stable bilayer. Other lipid mixtures can be used as long as there is a proper balance of negatively charged and zwitterionic lipids. We have shown bilayer formation from DOPC and DOPS vesicles containing charged lipids from 50 to 70 % molar ratios [17]. When more than 70 % or less than 50 % of charged lipids were used no bilayer was obtained[17]. The presence of charged lipids is fundamental as they interact strongly with the amines of PAH leading to vesicle rupture and fusion. However, for vesicles with higher amount of charged lipids, the interaction with PAH is so strong that the adsorbed vesicles have restricted mobility and they are not able to

rearrange on the surface of the PEMs; thus the presence of zwitterionic lipids is also important as these can rearrange and cover free space on the PEMs, which is necessary for fusion.

We have also shown that the formation of a bilayer is therefore associated with hydrogen bonding interactions between the lipids and PAH with some additional attractive electrostatic interactions[17]. In case of pure DOPC lipids, the choline group, which is positively charged, exercises a certain repulsion to the amine groups of PAH, which is against the lipid assembly. There must be some electrostatic contribution that favors the deposition from bulk. However this should not be strong, otherwise vesicles will rapidly cover the surface and there will not be enough free space for them to rearrange, fuse and form a bilayer, remaining adsorbed or as partially fused vesicles on the PEMs[18]. Such a condition is possible using PBS buffer but not with NaCl at a same ionic strength. At NaCl concentration of 150 mM, the vesicles adsorb to the PEM surface without forming a bilayer[18]. The reason why a bilayer is formed on top of PAH/PSS multilayers in PBS depends on the strong complexation of the phosphate ions in PBS to the primary amine groups of PAH, which leads to an overcompensation of the surface charge. Particles coated with PAH/PSS multilayers in PBS show a zeta potential of around zero.

The presence of primary amines with a strong interaction with phosphate groups seems to be the key point in the formation of bilayers on top of PAH/PSS. PAH can be assembled with other polyanions to form polyelectrolyte multilayers, e.g., polyacrylic acid (PAA) or alginic acid sodium salt (Alg). We decided to study the bilayer formation on PEMs with PAH as top layers but with PAA or Alg as polyanions. Despite the last layer was the same as for PAH/PSS multilayers, to our surprise we were did not obtain a bilayer using the same conditions that render the formation of a bilayer on top of PAH/PSS. PEMs properties are a result of the properties and interactions of both polycations and polyanions that form the multilayer. It is likely that PSS interacts differently with PAH from PAA and Alg and as a consequence, the interaction of the amine groups of PAH with the phospholipids is also affected. PAA and Alg are

weak polyelectrolytes, whose charge is influenced by the pH and thus by the interaction with PAH while PSS is a strong polyelectrolyte, with a pK of 1.

The aim of this work is to study in more detail the impact of polyanion variations on PEMs with PAH as top layer and thus on the formation of a lipid bilayer. Quartz crystal microbalance with dissipation (QCM-D) and fluorescence recovery after photobleaching (FRAP) measurements are applied to evaluate the bilayer formation from 50:50 molar ratio DOPC:DOPS vesicles hydrated with PBS on PAH/PAA and PAH/Alg multilayers. X-ray photoelectron spectroscopy (XPS) and zeta potential measurements are applied to characterize the interaction of amine groups of PAH with the phosphate ions in PBS.

Experimental Methods

Materials. Poly(allylamine hydrochloride), (PAH, Mw 15 kDa), poly(styrene sulfonate sodium salt), (PSS, Mw 70 kDa), Alginic acid sodium salt (Alg, Mw 10 – 600 kDa), poly(acrylic acid) solution in water 35 wt % (PAA, Mw 100 kDa), phosphate buffered saline (PBS), sodium chloride (NaCl) and chloroform anhydrous (> 99%) were obtained from Sigma-Aldrich. The phospholipids 1,2-Dioleoyl-sn-glycero-3-phosphocholine (DOPC, 10 mg/ml in chloroform), 1,2-dioleoyl-sn-glycero-3-phospho-L-serine (DOPS, sodium salt, 10 mg/ml in chloroform), chain-labeled 18:1-12:0 NBD-PC and 18:1-12:0 NBD-PS were purchased from Avanti Polar Lipids, Inc. Ethanol absolute (99,9 % HPLC) was obtained from Scharlau S.A.

Methods

Preparation of Vesicles. Small unilamellar vesicles (SUVs) were obtained by mixing negatively charged and zwitterionic phospholipids, DOPS and DOPC, respectively, at a 50:50 molar ratio from their stock solutions in chloroform (10 mg ml^{-1}) to a final concentration of 0.5 mg ml^{-1}. The mixture was dehydrated with an argon stream forming a thin lipid film and incubated under

vacuum afterwards for at least 1 hour to remove any remaining solvent. The lipid film was then rapidly hydrated with PBS 10 mM (pH 7.4) forming multilamellar vesicles, which resulted in SUVs of 100 nm sizes after extrusion through a 50 nm polycarbonate membrane. For FRAP experiments, 1 % of fluorescently labelled NBDPC:NBDPS lipids at 0.5:0.5 molar ratio was added to the initial lipid mixture.

QCM-D Measurements. QCM-D measurements were conducted with an E4 QCM-D at 23 ^{o}C employing SiO_2 coated (50 nm) quartz crystals (5 MHz) from Q-Sense. Initially the crystal was exposed to Milli-Q water for 10 min, for another 10 min to 0.5 M NaCl and then 11 layers of PEs were assembled in acetate buffer with 0.2 M NaCl (pH 5.6) at 1 mg ml^{-1} in the QCM-D chamber. For each layer deposition, PE solutions were flowing in the chamber for 10 – 20 min until stable values for the frequency were reached. Every deposited layer was then rinsed with the buffer. The last deposited layer was always PAH. When the PEM was completed, the chamber was rinsed with PBS. Then, the dispersion of SUVs in PBS (0.1 mg ml^{-1}) was injected into the chamber and flowed through the chamber for 10 min, until a stable frequency value was reached. Surplus or non-adsorbed vesicles were removed by rinsing with the buffer solution without SUVs for another 10 – 15 min.

FRAP Measurements. FRAP measurements were performed with a Zeiss LSM 510 confocal laser scanning microscope. For the measurements, PEMs and SUVs were assembled on top of glass (SiO_2) surfaces of 24 mm diameter by dipping, employing the same times for the assembly steps as for the QCM-D experiments. For FRAP measurements, vesicles with a 50:50 molar composition DOPC:DOPS were labelled, including a 0.5 % of labelled DOPC and a 0.5 % of labelled DOPS. We included both labelled DOPC and DOPS to have more realistic values for the diffusion, averaging the diffusion of DOPC and DOPS, which can be quite different on the PEMs.

FRAP measurements were performed as described by Axelrod et al.[19], Soumpasis et al.[20] and Lopez et al.[21] who developed a simple method based on theoretical and practical guidelines for the performance of FRAP measurements and for the analysis of the obtained data in order to extract mobile lipid fractions and diffusion coefficients. First, a round spot of 22 μm diameter was photobleached with an Argon laser during 5 s while at the same time a non–bleached spot of the same size was taken into account as a reference.

For the theoretical analysis of the experimental data, the fluorescence recovery is defined as

$$f(t) = \frac{F(t) - F(0)}{F(i) - F(0)} \quad \text{(Eq. 1)}$$

where $F(t)$ is the fluorescence recovery in the bleached area after photobleaching at time *t*, $F(0)$is the fluorescence intensity in the bleached area at $t = 0$ after photobleaching and $F(i)$ is the normalized fluorescence intensity in the non-bleached spot. By applying this equation, the fluorescence intensity drift of the whole sample due to the photobleaching during the scanning process is normalized. For the calculation of D, a fitting of $f(t)$ is required:

$$f(t) = exp\left(-2\frac{\tau_D}{t}\right)\left[I_0\left(2\frac{\tau_D}{t}\right) - I_1\left(2\frac{\tau_D}{t}\right)\right] \quad \text{(Equation 2)}$$

I_0 and $I_1$are modified Bessel functions, τ_D is the characteristic diffusion time calculated from

$$\tau_D = \frac{\omega^2}{4D} \quad \text{(Equation 3)}$$

where D is the diffusion coefficient and ω is the radius of the bleached area at zero time. Finally, the mobile fraction is calculated using the Eq. 14.

$$\boldsymbol{M} = \frac{[\boldsymbol{F}(\infty) - \boldsymbol{F}(\mathbf{0})]}{[\boldsymbol{F}(\boldsymbol{i}) - \boldsymbol{F}(\mathbf{0})]} \quad \text{(Equation 4)}$$

XPS Measurements. XPS experiments were performed in a SPECS Sage HR 100 spectrometer with a non-monochromatic X-ray source (Aluminum Kα line of 1486.6 eV energy and 300 W), placed perpendicular to the analyzer axis and calibrated using the $3d_{5/2}$ line of Ag with a full width at half maximum (FWHM) of 1.1eV. The selected resolution for the spectra was 10 eV of Pass Energy and 0.15 eV/step. All measurements were made in an ultra-high vacuum (UHV) chamber at a pressure around $5 \cdot 10^{-8}$ mbar. An electron flood gun was used to neutralize for charging.

For the fitting of the P 2p spectra, Gaussian-Lorentzian functions were used (after a Shirley background correction) where the FWHM of all the peaks were constrained while the peak positions and areas were set free.

ζ-Potential Measurements. ζ - potential measurements were conducted with a Zetasizer (Malvern, UK) in a disposable folded capillary cell at 23 ^{o}C and a cell drive voltage of 40 V. All parameters were set in automatic mode. PEMs of PAH/PSS, PAH/Alg and PAH/PAA were assembled on top of 1 μm SiO_2 particles. SiO_2 particles, 1 mg ml^{-1}, were initially suspended in acetate buffer with 0.2 M NaCl. Then, the particles were incubated at the respective polyelectrolyte solution (1 mg ml^{-1} in acetate buffer with 0.2 M NaCl, pH 5.6) for 15 min. The procedure was repeated for every layer deposition for the assembly of 11 layers. In between polyelectrolyte depositions, three washing steps with the acetate buffer (pH 5.6) were performed via centrifugation. After the last washing step, samples were dispersed in different solutions; H_2O, NaCl 10 mM, NaCl 150 mM, PBS 10 mM, Na_2HPO_4 10 mM or KH_2PO_4 2 mM and were kept shaking for 5 min. Finally, each sample was washed 3 times with the same solutions and their surface charge was characterized. Standard deviation errors were taken out of 3 repetition measurements for each sample.

Results and Discussion

The assembly of a lipid bilayer on top of PEMs that have PAH as top layer was studied by depositing SUVs of DOPC:DOPS in a 50:50 molar composition, hydrated in PBS 10 mM.

In **Figure 1a** we show the assembly of SUVs on top of $(PAH/PSS)_{5.5}$ that results in the formation of a bilayer. This can be concluded from the changes in frequency and dissipation, which are characteristic of a bilayer formation[16,17,22]. An initial decrease in frequency is observed during vesicle adsorption, followed by a rapid increase as a consequence of the rupture of the vesicles that liberated the entrapped solution and finally the frequency reached a plateau when the ruptured vesicles were fused forming a bilayer. Dissipation curves can be described in a similar way. Dissipation increased when the vesicles were assembled onto the PEMs as vesicles are soft and their lipid membranes can bend and oscillate while they are deposited on the PEMs. As the vesicles rupture and start to fuse, dissipation decreased to finally reach a plateau when the fusion is completed. The fused bilayer is in a more solid like configuration and is less dissipative than in the case of the non-ruptured vesicles[23]. The total frequency shift and dissipation variation for the bilayer were $\Delta f = 27$ Hz and $\Delta D = 0.3 \times 10^{-6}$ dissipation units, respectively. In **Figure 1b** we can observe the frequency and dissipation changes following the deposition of DOPC:DOPS SUVs on top of $(PAH/Alg)_{5.5}$. Although frequency and dissipation curves follow a similar trend to the one obtained when a bilayer is formed, we cannot claim the formation of one as the total frequency shift is $\Delta f = 70$ Hz while was $\Delta D = 11 \times 10^{-6}$. The QCM-D plot suggests a strong interaction between the SUVs and PEM surface as the frequency decreased immediately to 80 Hz after SUVs deposition, and then increased again 10 Hz, which hints at partial rupture of the vesicles. Despite the vesicle rupture hinted by the decrease in frequency, followed by an increase, the total frequency difference is significantly larger than that expected for a bilayer formation, indicating that the lipid vesicles remain as such, at least partially, on the PEM surface. Substitution of the negatively charged polyelectrolyte with PAA resulted in a similar situation (**Figure 1c**). In this case the frequency difference was $\Delta f = 71$ Hz while the dissipation

changed 3 x 10^{-6} units, suggesting that the deposited vesicles have a more restricted mobility than in the case of $(PAH/Alg)_{5.5}$ where dissipation was higher following vesicles adsorption. FRAP measurements were conducted on fluorescently labelled SUVs deposited on top of $(PAH/PSS)_{5.5}$. FRAP measurements confirmed the lipid bilayer formation in agreement with QCM-D measurements (**Figure 2a**). The recovery was complete after 2.93 min as it can be distinguished by the respective recovery plot in **Figure 2a** and the diffusion coefficient calculated from the fitting of the experimental data to **Equation 2,** which was 9.2 x 10^{-9} cm^2 s^{-1}. This value is in accordance with diffusion coefficient values reported for lipid bilayers[24,25]. Diffusion coefficient and mobile fraction values are listed in **Table 1**.

In the case of $(PAH/Alg)_{5.5}$, the recovery of fluorescence was not complete as is illustrated in **Figure 2b**. The diffusion coefficient was low; D = 0.36 x 10^{-9} cm^2 s^{-1} confirming that the vesicles were not fully fused as was hinted from the QCM. FRAP experiments on SUVs deposited on $(PAH/PAA)_{5.5}$ (**Figure 2c**) revealed the formation of bilayer patches with different fluorescence intensity (**Figure 3**). When regions with lower fluorescence intensity were photobleached, no recovery was observed. The lack of recovery can be explained as the result of the presence of SUVs that did not rupture and they remained adsorbed on the PEMs. As the vesicles are not interconnected the bleached lipids cannot be exchanged by non-bleached lipids. When the higher fluorescence intensity region was photobleached, a fluorescence recovery was observed afterwards; however, the recovery was not complete (M = ~ 0.89) and the diffusion coefficient (**Table 1**) was lower than for the bilayer formed on $(PAH/PSS)_{5.5}$, suggesting as well, partially fused SUVs. We can conclude from the FRAP experiments that SUVs are only partially fused on PAH/PAA PEMs in agreement with QCM-D data.

The absence of the formation of a complete bilayer on PAH/Alg or PAH/PAA, despite PAH is in all cases the last layer, can be due to either a different interaction of the PAH with the phospholipids when the underlying polyanion is not PSS or to the different properties of the films, i.e., different mechanical properties. PEMs made upon PAH/PSS are very stiff with an

elasticity modulus of around 500 MPa, while the other PEMs must have an elasticity modulus of the order of hundreds of kPa. Both possible scenarios are a consequence of the different interaction of the polyanions with PAH[26,27].

To evaluate the role of the surface chemistry of the top layers in bilayer formation, PAH/PSS PEMs were prepared with 1 or 2 layers of Alg or PAA deposited on top. The idea behind these experiments was to fabricate PEMs with the bulk characteristics of PAH/PSS, with different surface chemistry by introducing Alg or PAA on their surface. To this regard the following PEMs were assembled: $(PAH/PSS)_{4.5}(PAH/Alg)$, $(PAH/PSS)_{3.5}(PAH/Alg)_2$, $(PAH/PSS)_{4.5}(PAH/PAA)$, $(PAH/PSS)_{3.5}(PAH/Alg)_2$. The reversal situation was also explored and PEMs with PAH/PSS on top of PAH/Alg and PAH/PAA were prepared with the following compositions: $(PAH/Alg)_{4.5}(PAH/PSS)$, $(PAH/Alg)_{3.5}(PAH/PSS)_2$, $(PAH/PAA)_{4.5}(PAH/PSS)$, $(PAH/Alg)_{3.5}(PAH/PSS)_2$. In these cases the mechanical properties of the PEMs should be those of PAH/PAA or PAH/Alg but the surface chemistry of that of PAH/PSS.

When SUVs were assembled on top of $(PAH/PSS)_{4.5}(PAH/Alg)$ (**Figure 4a**), the frequency decreased as a consequence of the adsorption of the vesicles, then increased, indicating rupture of the vesicles, and finally remained stable suggesting the formation of a bilayer. Although the total frequency shift was 37 Hz, higher than that expected for a bilayer, the frequency and dissipation trend is typical of a bilayer[22], while after rinsing with the buffer or water, the frequency hardly changed, indicating the presence of a continuous and stable membrane. On the contrary, when SUVs were deposited onto the same film, with the last 2 Alg polyanion layers, (**Figure 4b**), the frequency showed rupture of vesicles. However, after rupture, there was a further decrease in frequency, resulting in a total shift of $\Delta f = 49$ Hz. This trend, together with the changes that occurred in frequency and dissipation during the final rinsing steps was similar to that obtained for the $(PAH/Alg)_{5.5}$ film, where there was a partial rupture of the vesicles. In the case of $(PAH/PSS)_{4.5}(PAH/PAA)$, **Figure 5a**, the difference of frequency was $\Delta f = 100$ Hz and there was no clear sign of vesicle rupture. In **Figure 6a**, the deposition of SUVs on top of

$(PAH/Alg)_{4.5}(PAH/PSS)$ is shown where frequency and dissipation curves indicated rupture and the formation of a bilayer (Δf = 37 Hz). The frequency slightly decreased after rupture and then remained stable for more than 30 min, and, after rinsing with NaCl and water, decreased another 10 Hz with the dissipation increasing slightly to 1 x 10^{-6} units. This could be interpreted as partial fusion of the SUVs which are swelling when the ionic strength is decreased. In the case of $(PAH/Alg)_{3.5}(PAH/PSS)_2$ (**Figure 6b**), no bilayer formation is observed. The difference in frequency is 40 Hz and, although there is no hint of rupture in the frequency changes, the dissipation showed a jump right after the SUVs deposition that could be related to the liberation of enclosed water, and thus to partial rupture of the vesicles.

The deposition of SUVs on top of the PEM films prepared with $(PAH/PAA)_{4.5}(PAH/PSS)$, did not result in a bilayer as can be distinguished in **Figure 7a**. The frequency decreased progressively to 47 Hz within 30 min and there was no hint of rupture. Dissipation increased slightly after SUVs adsorption and then decreased and remained stable after rinsing with PBS, while it hardly changed after the final rinsing steps. Finally, by the deposition of SUVs on top of $(PAH/Alg)_{3.5}(PAH/PSS)_2$, we observed partial rupture of vesicles as can be seen in **Figure 7b**. The total frequency shift was 54 Hz. The frequency hardly changed after rinsing with NaCl or water, showing no or limited swelling of the adsorbed vesicles and the bilayer patches.

The results from the assembly of SUVs on PEMs combining PAH/PSS, with Alg as the underlying layer before the outermost PAH layer, hint that the mechanical properties play an important role on the formation of the bilayer; In this case the film must have approximately the mechanical properties of the PAH/PSS differing only in the chemistry of the polyanion layer below the top polyelectrolyte layer. However, if this were the case, bilayer formation should be hindered for PAH/Alg PEMs with PAH/PSS as top deposited layers, as the film has basically the mechanical properties of PAH/Alg, but occurs the opposite. On the other hand, the experiments combining PAH/PSS and PAH/PAA multilayers did not result in bilayer formation in none of the cases.

A possible explanation for these results is that since there is normally interdigitation between layers in PEMs, the last PAH layer interacts in both cases with PSS and alginate, and, therefore, there is not much difference for the lipid assembly between the PEMs of PAH/Alg with PAH/PSS as top layers and PAH/PSS with PAH/Alg as top layers. The same may be occurring for PAH/PSS and PAH/PAA. If so, the composition of the top layers would be responsible for the bilayer formation.

In a previous work, we have shown that the interaction of phosphate ions with PAH is fundamental for achieving a bilayer formation on the PAH/PSS PEMs[28]. Therefore, we decided to study the influence of PBS on PAH/Alg and PAH/PAA. ζ–Potential measurements were conducted on colloidal particles coated with 11 layers of PAH/PSS, PAH/Alg and PAH/PAA in order to reveal the changes in surface charge after incubation in NaCl 10 mM and 150mM, PBS 10 mM and in the salts contained in the PBS buffer at the same molarities; Na_2HPO_4 10 mM, KH_2PO_4 2 mM, Na_2HPO_4 10 mM/ NaCl 150 mM and KH_2PO_4 2 mM/ NaCl 150 mM. Results (**Table 2**) showed that even though the last deposited layer was always the positively charged PAH, the potential was affected by the negatively charged polyelectrolyte. In NaCl 10 mM the potential for $(PAH/PSS)_{5.5}$ was 47 mV while that for $(PAH/Alg)_{5.5}$ was 34 mV and that for $(PAH/PAA)_{5.5}$ was 43 mV.

In all cases the potential diminished significantly in the presence of PBS reaching negative values, which however, varied for each polyanion (**Table 2**). In the case of PAH/PSS the potential was almost zero and for PAH/Alg and PAH/PAA was negative; - 15 mV and - 12 mV, respectively. In the presence of the dibasic phosphate salt (Na_2HPO_4, 10 mM) the surface charge was also negative around -15.1 ± 1.6 mV, lower than for PBS. It was interesting that even though in the case of the monobasic phosphate salt (KH_2PO_4, 2 mM) the potential decreased, it did not decrease significantly and the surface charge of all samples remained positive, hinting that PAH mostly interact with the dibasic phosphate. Accordingly, samples in Na_2HPO_4 10 mM/ NaCl 150 mM displayed potentials close to the ones obtained for PBS.

XPS measurements were conducted on the three PEMs after exposing them to PBS. Results showed that the phosphate interacted strongly with the PAH and that this interaction was affected by the change of polyanion (**Figure 8**). The PAH/Alg presented a relative phosphorous content of around 0.9 atom %, compared to the PAH/PSS with 1.0 atom %. PAH/PAA showed the highest relative content of phosphorous, around 1.9 atom %. In both cases, the P $2p_{3/2}$ peak attributed to phosphate bonds is shifted to lower binding energies, at around 132.4 eV. This energy value corresponds to the energy of dibasic phosphate ions (**Figure S1**) and would indicate that PAH assembled with Alg and PAA are preferentially interacting with the dibasic phosphates (PO_4^{2-}). On the other hand, the energy of the phosphates bound to PAH/PSS corresponds to the monobasic phosphate salts (**Figure S1**). The calculated ratio of phosphates to the number of amines on the surface of each sample (**Table 3**) show, in the case of PAH/PSS, that there was half complexation of the amines. For PAH/Alg, the complexation was 35 atom % with the N of PAH on the surface of the film. For PAH/PAA, this value increases to an 88 atom %. These values are calculated considering that all the phosphate groups are complexed with the amines of the top layer. XPS profiles of phosphate along the PEMs (not shown), demonstrate that there are almost no phosphate groups in the film interior.

The negative potential of the PAH/Alg and PAH/PAA in PBS indicates a net negative charge on the PEMs. Despite the negative charge of the PEM surface, not all amine groups are interacting with phosphate groups as we observed from XPS. Therefore, on the PEM surface there will be negative charges from the phosphate, but also charged or neutral amino groups available. The negative charges should induce repulsion of the vesicles, but, when the vesicles approach to the areas where the amines are not complexed with the phosphates, they can interact with the free amino groups. In the ionic strength conditions used in this study, the Debye length should be approximately 1 nm. The vesicles can come close to the PEM surface up to this distance without facing repulsion. Besides, if the vesicles find positively charged or non-charged amines on the surface, they will adsorb and even partially ruptured. We can assume a homogenous distribution

of amines complexed with the phosphate groups and not-complexed amines. Vesicles will interact with amines non complexed with phosphate ions, which can lead to their rupture and partial fusion, but will face repulsion from the amines complexed with the phosphate groups that should prevent spreading. This would explain the formation of bilayer patches on the PEMs, especially in the case of PAH/Alg. It is worth noting that in the case of PAH/PAA, where there is a larger complexation with the phosphate groups, there are more vesicles assembled than bilayer patches as can be deduced from the QCM-D and FRAP measurements. This was well correlated with the reduced number of amine groups available to interact with the phospholipid vesicles. The preferential interaction of PAH/PSS and PAH/Alg with monobasic phosphates and PAH/PAA with dibasic phosphates, can be explained by the degree of protonation of the PAH as a consequence of the interaction with the polyanions in the neutral environment of PBS (pH 7.4). PAA and Alg are both weak polyelectrolytes with carboxylate groups that dissociate and can transfer protons to PAH increasing the PAH protonation. On the other hand in the same conditions, PSS is fully dissociated. Therefore, we can expect a lower protonation for PAH/PSS than for PAH/PAA and PAH/Alg at neutral pH values.

Conclusions

The results of this work show that the assembly of a bilayer on top of a polyelectrolyte multilayer is a complex process, not only ruled by the surface chemistry of the multilayer, but rather, by the composition of the PEM and the interactions between polyanions and polycations. Our results show that indeed the nature of the polyanion in the PEM fine-tuned the interaction of the PEMs with phosphate ions and phospholipids. We have observed that in the case of PAH/PSS multilayers in presence of PBS, the PAH, top layer, form complexes with monobasic phosphate ions through hydrogen bonding, rendering the surface with neutral charge, despite that not all amines of the PAH layer are complexed. In these conditions, the electrostatic interaction of the PEM with the vesicles is weak, but can form hydrogen bonding with the amines of PAH,

and a bilayer is formed. For the case of Alg or PAA as polyanions, we observe the complexation of the amines of PAH with dibasic phosphate ions that render the surface of the PEMs negatively charged. This negative charge should induce the repulsion of the vesicles, since these are negative as well. However, despite the overall negative charge of the PEM, not all amine groups form complexes with phosphate; they can remain either positively charged or not charged, and can therefore interact with proximal vesicles to form bilayer patches with non-fused vesicles.

Supporting Information.

XPS spectra of the monobasic and dibasic phosphate salts included in phosphate buffered saline are provided as **Supporting Information.**

Acknowledgments

This work was supported by the European Commission in the framework of FP7 PEOPLE-2013 Project HIGRAPHEN Proposal No. and the FP7 ERANET 2014 FATENANO, including support from the U. S. National Science Foundation (CBET-1530790). The authors also acknowledge the project MAT2013-48169-R from the Spanish Ministry of Economy (MINECO).

Figures

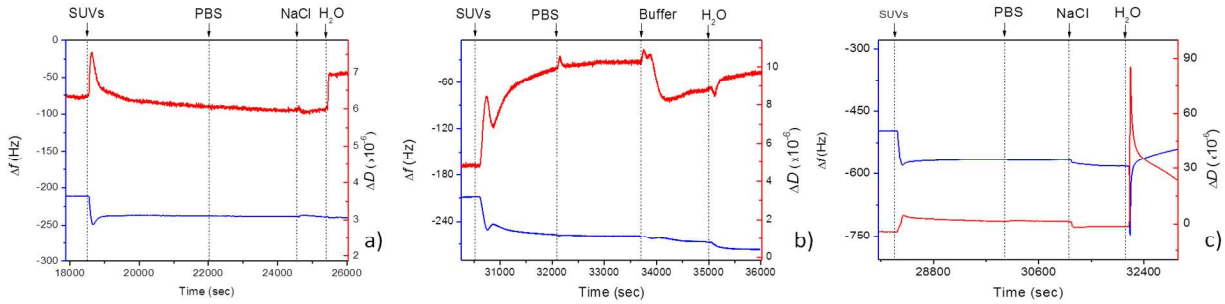

Figure 1 QCM-D curves of frequency (blue line) and dissipation (red line) following the deposition of DOPC:DOPS SUVs on top of a) $(PAH/PSS)_{5.5}$, b) $(PAH/ALG)_{5.5}$ and c) $(PAH/PAA)_{5.5}$ multilayer cushions.

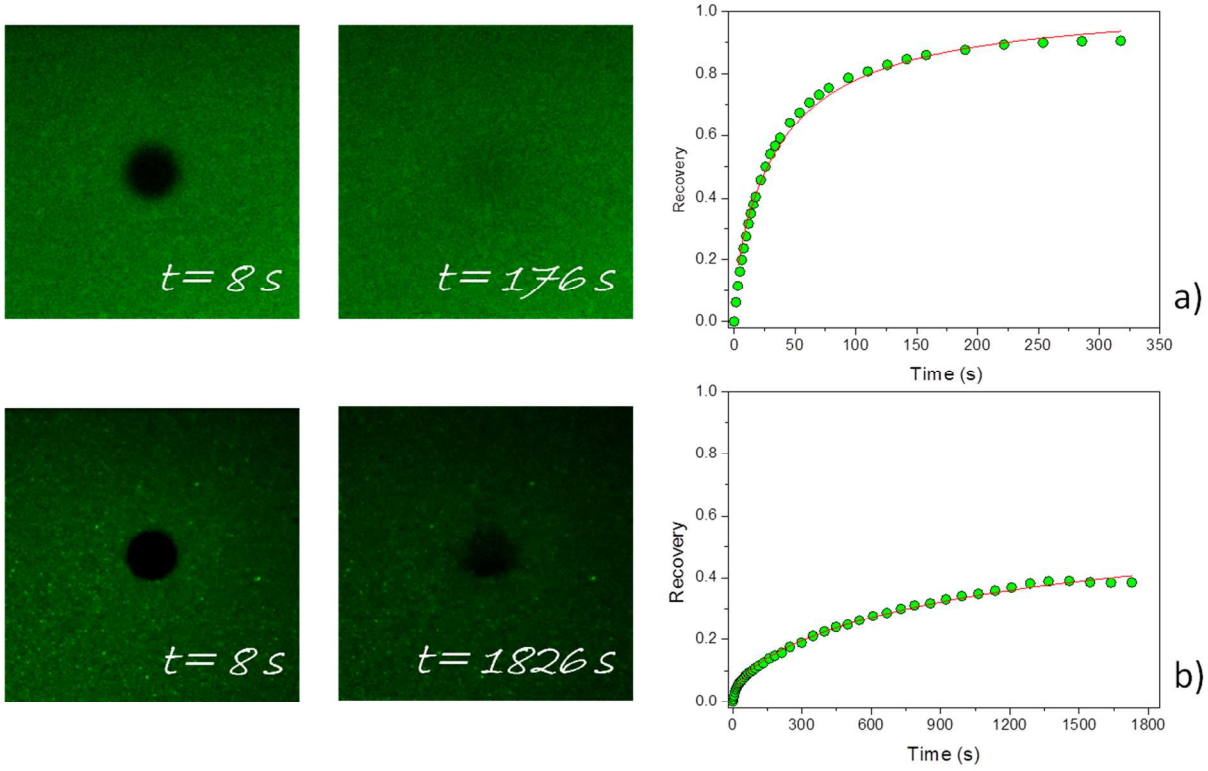

Figure 2 Fluorescence images after photobleaching and the respective fluorescence recovery curves obtained by the deposition of DOPC:DOPS labelled with 0.5:0.5 NBDPC:NBDPS fluorescent SUVs on top of a) $(PAH/PSS)_{5.5}$ and b) $(PAH/ALG)_{5.5}$ multilayer cushions.

Table 1 Mobile fraction and diffusion coefficient values obtained from the deposition of 50:50 molar ratio DOPC:DOPS SUVs on top of different PEM supports.

Sample	M	D (10^{-9}cm^2 s^{-1})
$(PAH/PSS)_{5.5}$	1.03 ± 0.019	9.2 ± 0.65
$(PAH/Alg)_{5.5}$	0.56 ± 0.017	0.36 ± 0.03

$(PAH/PAA)_{5.5}$	0.89 ± 0.007	7.7 ± 0.27

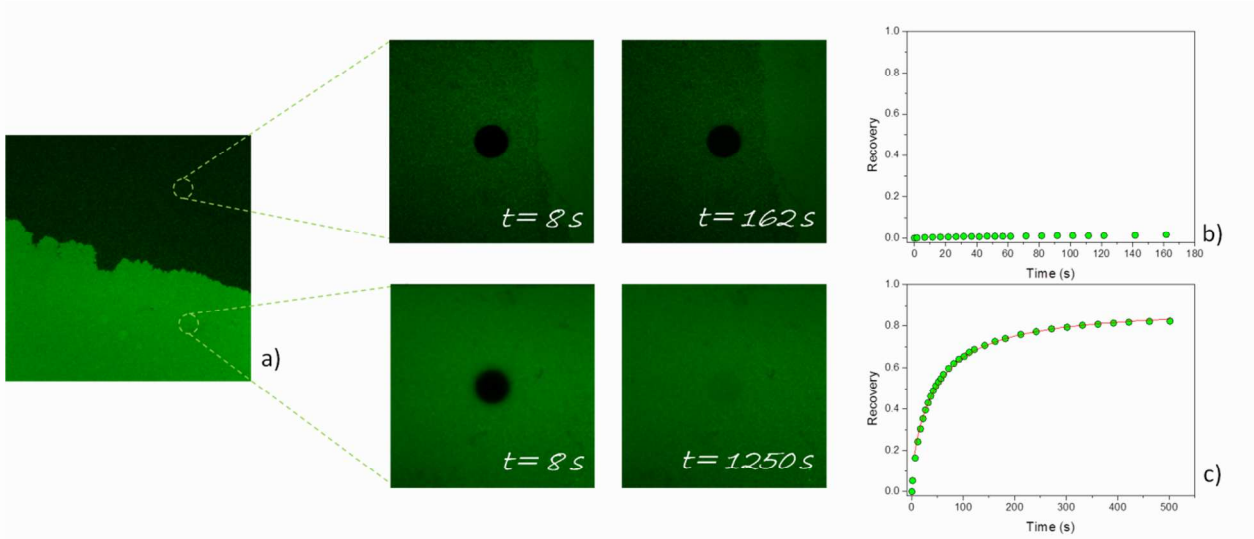

Figure 3 a) Ffluorescence image, of DOPC:DOPS SUVs, labelled with 0.5:0.5 NBDPC:NBDPS, adsorbed on top of $(PAH/PAA)_{5.5}$. b) Confocal Microscopy images and the respective fluorescence recovery curves after photobleaching from a region with low fluorescence intensity and c) from a region with higher fluorescence intensity.

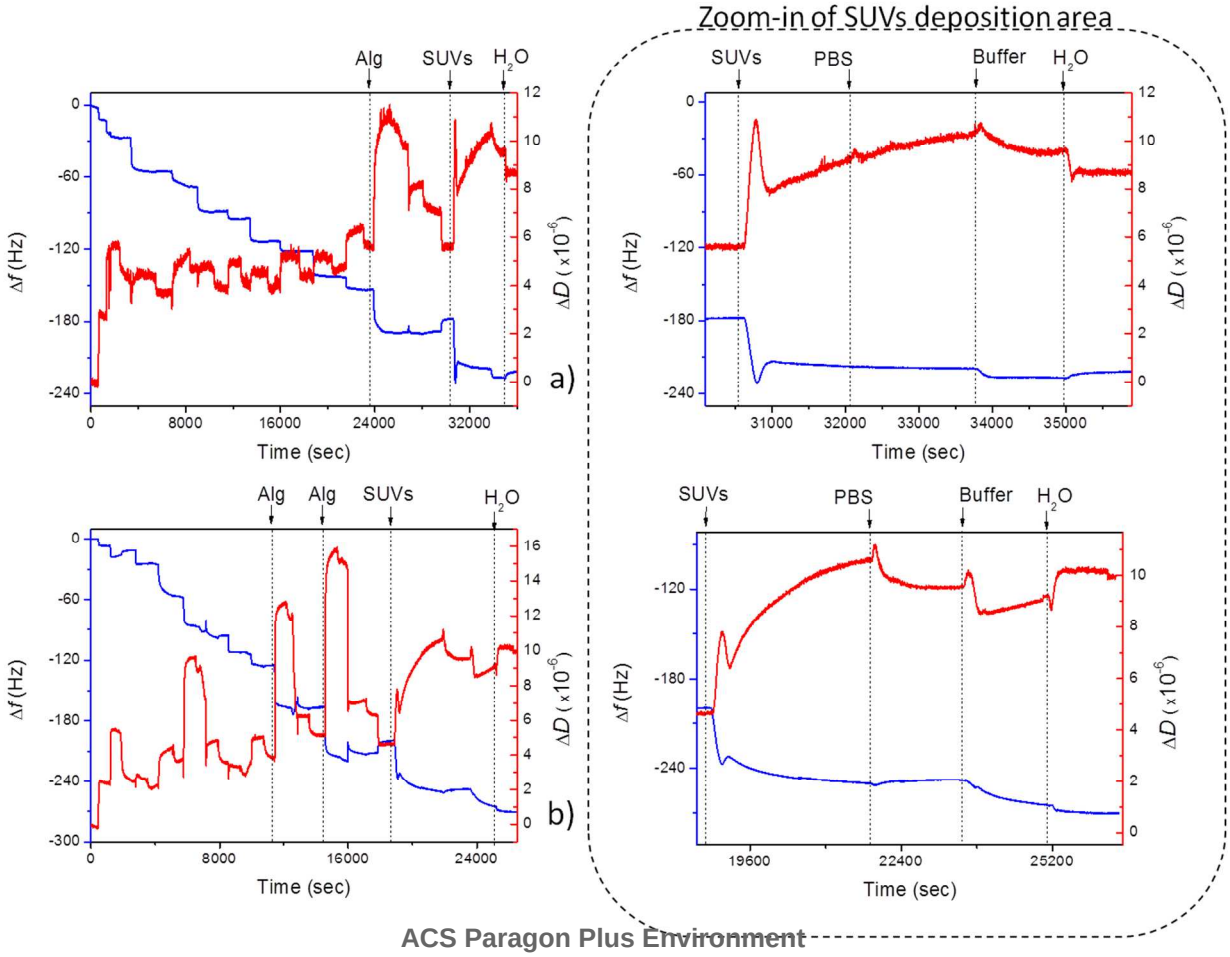

Figure 4 QCM-D curves of frequency (blue line) and dissipation (red line) tracing the deposition of DOPC:DOPS SUVs on top of a) $(PAH/PSS)_{4.5}(PAH/Alg)$ and b) $(PAH/PSS)_{3.5}(PAH/Alg)_2$ multilayer cushions.

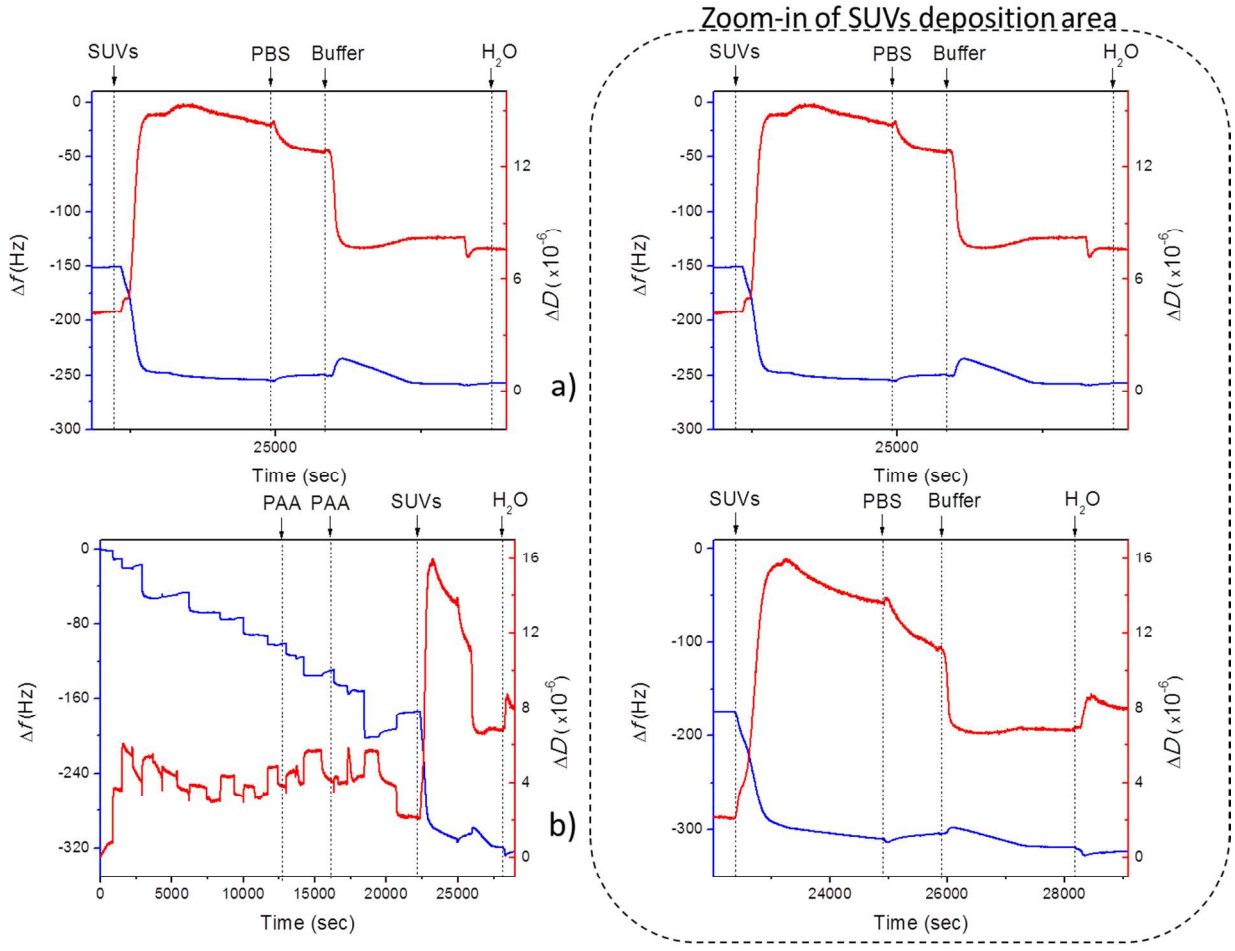

Figure 5 QCM-D curves of frequency (blue line) and dissipation (red line) tracing the deposition of DOPC:DOPS SUVs on top of a) $(PAH/PSS)_{4.5}(PAH/PAA)$ and b) $(PAH/PSS)_{3.5}(PAH/PAA)_2$ multilayer cushions.

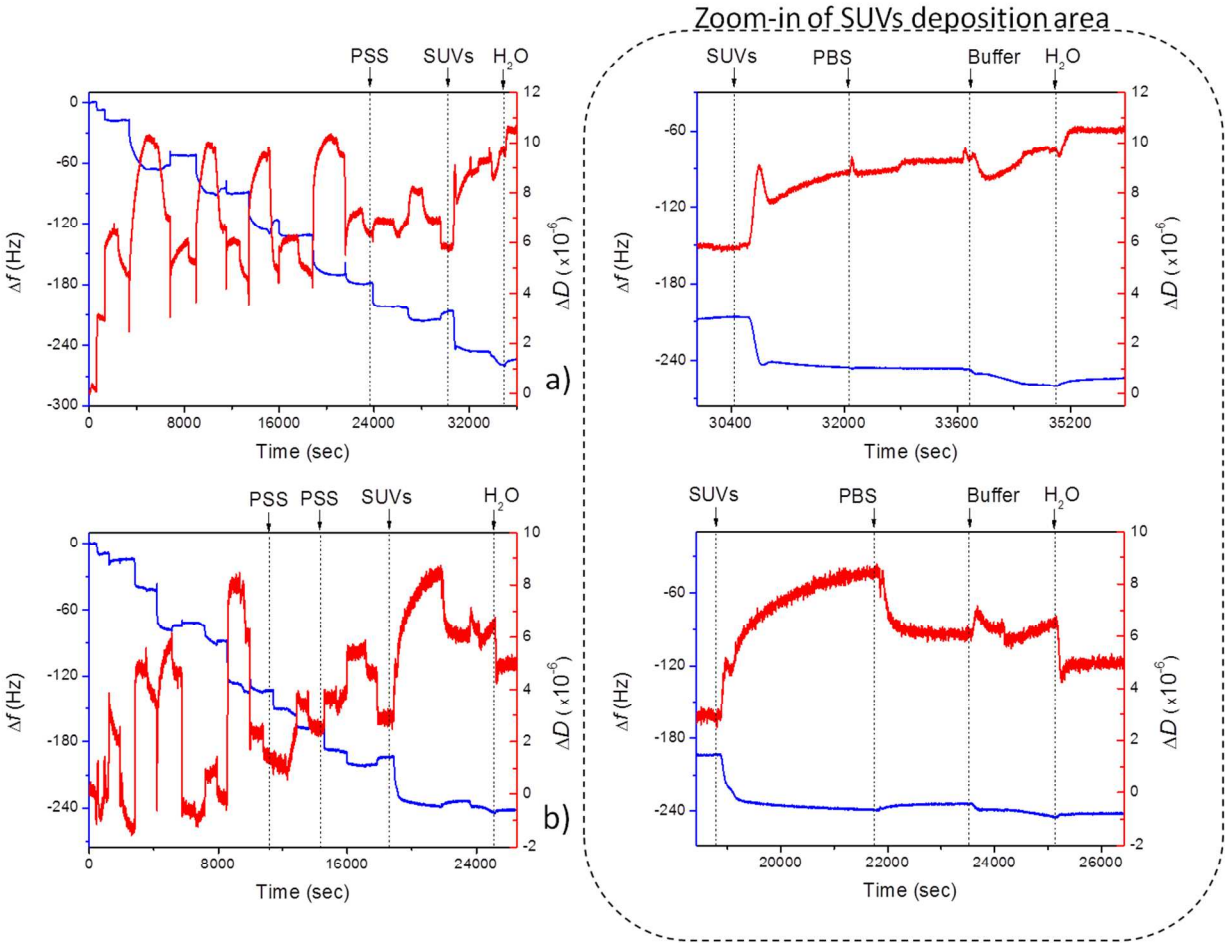

Figure 6 QCM-D curves of frequency (blue line) and dissipation (red line) obtained by the deposition of DOPC:DOPS SUVs on top of a) $(PAH/Alg)_{4.5}(PAH/PSS)$ and b) $(PAH/Alg)_{3.5}(PAH/PSS)_2$ multilayer cushions.

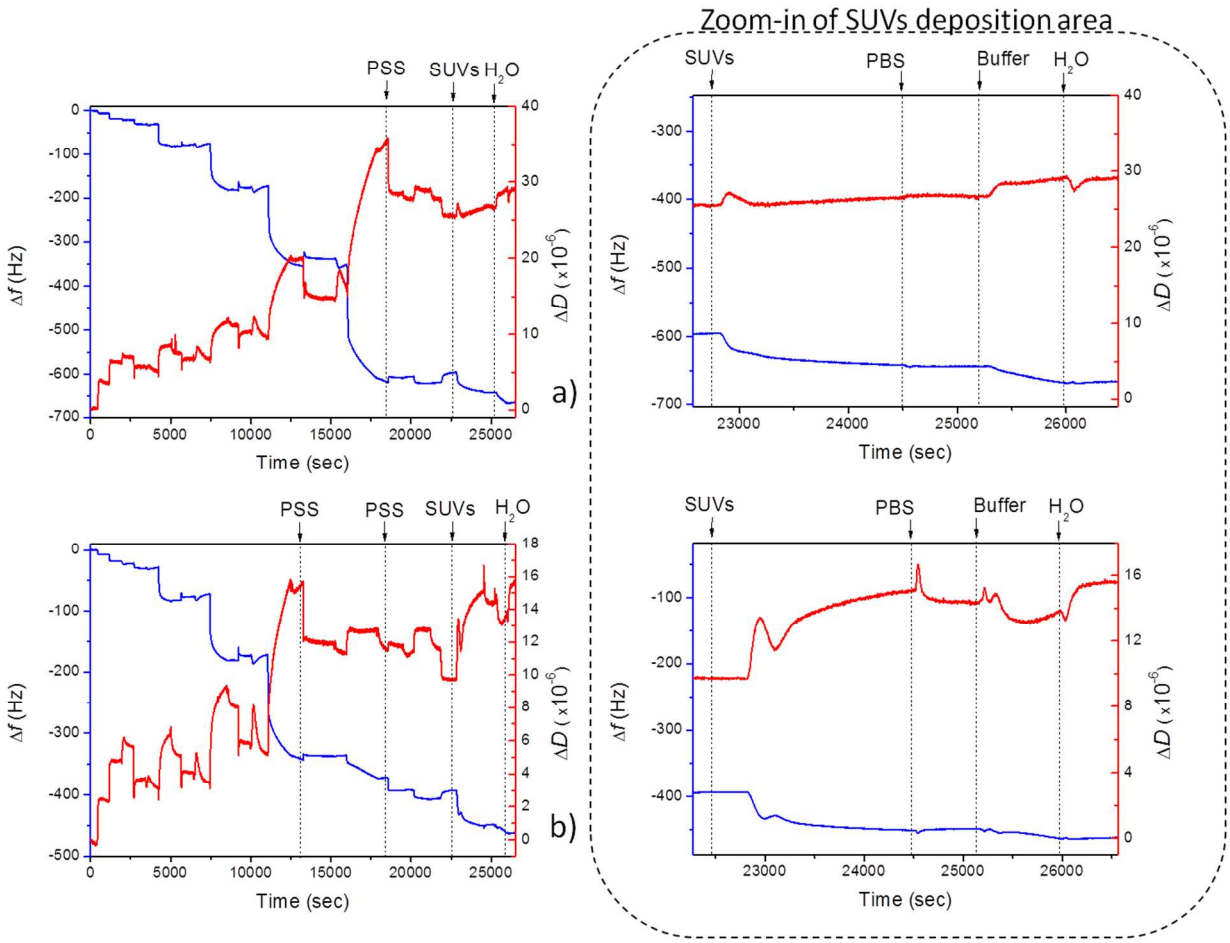

Figure 7 QCM-D curves of frequency (blue line) and dissipation (red line) tracing the deposition of DOPC:DOPS SUVs on top of a) $(PAH/PAA)_{4.5}(PAH/PSS)$ and b) $(PAH/PAA)_{3.5}(PAH/PSS)_2$ multilayer cushions.

Table 2 Zeta potential values of the $(PAH/PSS)_{5.5}$, $(PAH/Alg)_{5.5}$ and $(PAH/PAA)_{5.5}$ PEM coated SiO_2 particles in different salt solutions, at 25 °C.

		ζ – potential (mV)		
Medium	**M (mM)**	**$(PAH/PSS)_{5.5}$**	**$(PAH/Alg)_{5.5}$**	**$(PAH/PAA)_{5.5}$**
NaCl	10	47.2 ± 0.4	33.7 ± 0.5	43.3 ± 3.0
NaCl	150	20 ± 1	13,4 ± 0,3	-3,1 ± 0,6
PBS	10	-1.33 ± 0.6	-14.5 ± 1.9	-12.2 ± 1.1
Na_2HPO_4	10	-15.1 ± 1.6	-21.9 ± 1.2	-22.1 ± 1.8
KH_2PO_4	2	35.9 ± 1.1	21.4 ± 0.1	5.8 ± 2.4
Na_2HPO_4 / NaCl	10/150	3.1 ± 0.1	-3.8 ± 0.1	-2.74 ± 1.0
KH_2PO_4 / NaCl	2/150	25.6 ± 0.5	1.3 ± 1.0	-3.8 ± 1.0

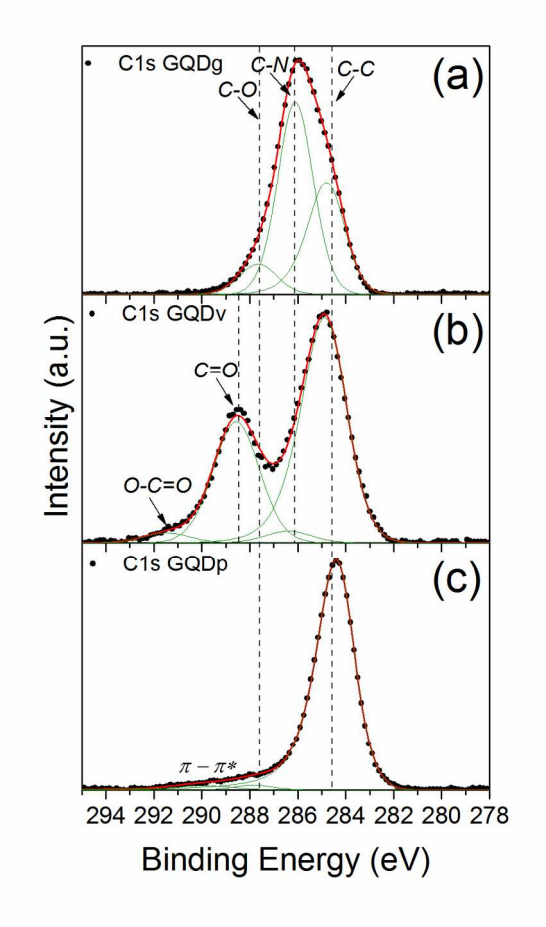

Figure 8 P 2p spectra of the a) $(PAH/PSS)_{5.5}$, b) $(PAH/Alg)_{5.5}$ and c) $(PAH/PAA)_{5.5}$ multilayers after rinsing with PBS.

Table 3 Chemical compositions of the samples obtained from the area of the high resolution photoelectron peaks, the N of the top layer and the relation of N with P for the top layer and the 3 last layers in terms of atom (at.)%.

Samples	N (at.%)	P (at.%)	C (at.%)	S (at.%)	N (at.%) **top layer**	Ratio N-P **top layer**	Ratio N-P **3 top layers**
PAH/PSS	9,6	**1,0**	81,4	8,0	1.9	52	26
PAH/ALG	12,7	**0,9**	86,5	0,0	2.5	35	18
PAH/PAA	11,3	**1,9**	86,6	0,2	2.3	84	42

References

(1) McConnell, H. M.; Watts, T. H.; Weis, R. M.; Brian, A. A. Supported Planar Membranes in Studies of Cell-Cell Recognition in the Immune System. *BBA - Rev. Biomembr.* **1986**, *864* (1), 95–106.

(2) Hladky, S. B.; Haydon, D. A. Ion Transfer across Lipid Membranes in the Presence of Gramicidin A. I. Studies of the Unit Conductance Channel. *BBA - Biomembr.* **1972**, *274* (2), 294–312.

(3) Cremer, P. S.; Boxer, S. G. Formation and Spreading of Lipid Bilayers on Planar Glass Supports. *J. Phys. Chem. B* **1999**, *103*, 2554–2559.

(4) Keller, C. A.; Glasmästar, K.; Zhdanov, V. P.; Kasemo, B. Formation of Supported Membranes from Vesicles. *Phys. Rev. Lett.* **2000**, *84* (23), 5443–5446.

(5) Richter, R. P.; Him, J. L. K.; Brisson, A. Supported Lipid Membranes. *Mater. Today* **2003**, *6* (11), 32–37.

(6) Allen, T. M.; Cullis, P. R. Liposomal Drug Delivery Systems: From Concept to Clinical Applications. *Adv. Drug Deliv. Rev.* **2013**, *65* (1), 36–48.

(7) Ryu, H.; Lee, H.; Iwata, S.; Choi, S.; Ki Kim, M.; Kim, Y.-R.; Maruta, S.; Min Kim, S.; Jeon, T.-J. Investigation of Ion Channel Activities of Gramicidin A in the Presence of Ionic Liquids Using Model Cell Membranes. *Sci. Rep.* **2015**, *5* (January), 11935.

(8) Jing, Y.; Trefna, H.; Persson, M.; Kasemo, B. Soft Matter Formation of Supported Lipid Bilayers on Silica : Liposome Size †. *Soft Matter* **2014**, *10*, 187–195.

(9) Rossetti, F. F.; Textor, M.; Reviakine, I. Asymmetric Distribution of Phosphatidyl Serine in Supported Phospholipid Bilayers on Titanium Dioxide. *Langmuir* **2006**, *22* (8), 3467–3473.

(10) Reviakine, I.; Brisson, A. Formation of Supported Phospholipid Bilayers from Unilamellar Vesicles Investigated by Atomic Force Microscopy. *Langmuir* **2000**, *16* (4), 1806–1815.

(11) Cassier, T.; Sinner, A.; Offenhäuser, A.; Möhwald, H. Homogeneity, Electrical Resistivity and Lateral Diffusion of Lipid Bilayers Coupled to Polyelectrolyte Multilayers. *Colloids Surfaces B Biointerfaces* **1999**, *15* (3–4), 215–225.

(12) Kügler, R.; Knoll, W. Polyelectrolyte-Supported Lipid Membranes. *Bioelectrochemistry* **2002**, *56* (1–2), 175–178.

(13) Singh, S.; Junghans, A.; Tian, J.; Dubey, M.; Gnanakaran, S.; Chlistunoff, J.; Majewski, J. Polyelectrolyte Multilayers as a Platform for pH-Responsive Lipid Bilayers. *Soft Matter* **2013**, *9* (37), 8938.

(14) Decher, G.; Hong, J. D.; Schmitt, J. Buildup of Ultrathin Multilayer Films by a Self-Assembly Process: III. Consecutively Alternating Adsorption of Anionic and Cationic Polyelectrolytes on Charged Surfaces. *Thin Solid Films* **1992**, *210–211*, 831–835.

(15) Decher, G.; Eckle, M.; Schmitt, J.; Struth, B. Layer-by-Layer Assembled Multicomposite Films. *Curr. Opin. Colloid Interface Sci.* **1998**, *3* (1), 32–39.

(16) Fischlechner, M.; Zaulig, M.; Meyer, S.; Estrela-Lopis, I.; Cuéllar, L.; Irigoyen, J.;

Pescador, P.; Brumen, M.; Messner, P.; Moya, S.; et al. Lipid Layers on Polyelectrolyte Multilayer Supports. *Soft Matter* **2008**, *4* (11), 2245–2258.

(17) Diamanti, E.; Cuellar, L.; Gregurec, D.; Moya, S. E.; Donath, E. Role of Hydrogen Bonding and Polyanion Composition in the Formation of Lipid Bilayers on Top of Polyelectrolyte Multilayers. *Langmuir* **2015**, *31*, 8623–8632.

(18) Diamanti, E.; Andreozzi, P.; Anguiano, R.; Yate, L.; Gregurec, D.; Politakos, N.; Ziolo, R. F.; Donath, E.; Moya, S. E. The Effect of Top-Layer Chemistry on the Formation of Supported Lipid Bilayers on Polyelectrolyte Multilayers: Primary versus Quaternary Amines. *Phys. Chem. Chem. Phys.* **2016**, *18* (47), 32396–32405.

(19) Axelrod, D.; Koppel, D. E.; Schlessinger, J.; Elson, E.; Webb, W. W. Mobility Measurement by Analysis of Fluorescence Photobleaching Recovery Kinetics. *Biophys. J.* **1976**, *16* (9), 1055–1069.

(20) Soumpasis, D. M. Theoretical Analysis of Fluorescence Photobleaching Recovery Experiments. *Biophys. J.* **1983**, *41* (1), 95–97.

(21) Lopez, A.; Dupou, L.; Altibelli, A.; Trotard, J.; Tocanne, J. F. Fluorescence Recovery after Photobleaching (FRAP) Experiments under Conditions of Uniform Disk Illumination. Critical Comparison of Analytical Solutions, and a New Mathematical Method for Calculation of Diffusion Coefficient D. *Biophys. J.* **1988**, *53* (6), 963–970.

(22) Keller, C. A.; Kasemo, B. Surface Specific Kinetics of Lipid Vesicle Adsorption Measured with a Quartz Crystal Microbalance. *Biophys. J.* **1998**, *75* (September), 1397–1402.

(23) Voinova, M. V.; Rodahl, M.; Jonson, M.; Kasemo, B. Viscoelastic Acoustic Response of Layered Polymer Films at Fluid-Solid Interfaces: Continuum Mechanics Approach. *Phys. Scr.* **1999**, *59* (5), 391–396.

(24) Przybylo, M.; Sýkora, J.; Humpolíčková, J.; Benda, A.; Zan, A.; Hof, M. Lipid Diffusion in Giant Unilamellar Vesicles Is More than 2 Times Faster than in Supported Phospholipid Bilayers under Identical Conditions. *Langmuir* **2006**, *22* (22), 9096–9099.

(25) Zhu, L.; Gregurec, D.; Reviakine, I. Nanoscale Departures: Excess Lipid Leaving the Surface during Supported Lipid Bilayer Formation. *Langmuir* **2013**, *29* (49), 15283–15292.

(26) Decher, G. Fuzzy Toward Mu Nanoassemblies : Layered Polymeric Ticom Posites Gero Decher. *Adv. Sci.* **1997**, *277* (5330), 1232–1237.

(27) Vinogradova, O. I.; Andrienko, D.; Lulevich, V. V; Nordschild, S.; Sukhorukov, G. B. Young's Modulus of Polyelectrolyte Multilayers from Microcapsule Swelling. *Macromolecules* **2004**, *37* (3), 1113–1117.

(28) Diamanti, E.; Muzzio, N.; Gregurec, D.; Irigoyen, J.; Pasquale, M.; Azzaroni, O.; Brinkmann, M.; Moya, S. E. Impact of Thermal Annealing on Wettability and Antifouling Characteristics of Alginate Poly-L-Lysine Polyelectrolyte Multilayer Films. *Colloids Surfaces B Biointerfaces* **2016**, *145*, 328–337.

TOC Graphic